24th INTERNATIONAL CONGRESS ON SOUND AND VIBRATION
23–27 July 2017, London

SURFACE WAVES DUE TO PERIODICALLY-SPACED STRIPS ON AN ACOUSTICALLY-HARD SURFACE

Alexander Stronach, Shahram Taherzadeh, Keith Attenborough

The Open University, School of Engineering & Innovation, Milton Keynes, UK
email: alex.stronach@open.ac.uk

Surface waves travelling at close to the speed of sound in air are created when the sound is incident near grazing angles near any rough, high impedance surface. It has been observed in laboratory measurements that the surface waves have greater magnitudes if the roughness spacing is regular rather than random. The creation of surface waves as well as the interference between direct and reflected sound results in characteristic excess attenuation spectra in which the reinforcement is more than 6dB at the surface wave frequencies. If the surface waves are subsequently absorbed then this offers a method of reducing the overall incident sound levels. Alternatively, the presence of surface waves can be used for signal enhancement in, for example, perimeter security applications. Point-to-point propagation over an array of regularly spaced rectangular strips produces surface waves. A series of systematic numerical and experimental investigations are reported into the influences of source-receiver geometry, strip height and strip width on the surface wave magnitude and frequency. Also, the influence of finite strip length and strip array depth have been investigated.
Keywords: Surface waves, roughness, boundary element method, excess attenuation.

1. Introduction

Analytical and experimental studies of sound propagating from a point source above air-filled porous media determine the existence of two types of surface wave. The first surface wave is associated with the elastic properties of the solid frame in poroelastic media and is similar in nature to the Rayleigh wave observed at the free boundary of an elastic solid [1,2]. The second is related to the pore structure of the medium. This is the dominant surface wave observed in an air-filled porous layer with a rigid frame. This second surface wave travels slower than the speed of sound in air and is associated with a surface impedance where the reactance is greater than the resistance. Vertical to and fro motion of air particles due to sound penetrating the surface couples with the to and fro horizontal motion of air particles due to sound travelling parallel to the surface. The resultant elliptical motion is associated with a surface wave which traps sound energy at certain frequencies close to the surface resulting in an enhancement greater than the 6dB associated with total reflection from an acoustically rigid surface.

Hutchinson-Howorth and Attenborough [3] carried out measurements over single and double lattice layers using tone bursts. They observed the surface wave contribution separated from the original impulse indicating that the surface wave travels slower than the speed of sound in air. Zhu *et al* [4] conducted measurements over a lattice and a mixed-impedance ground surface composed of strips to investigate the passive amplification of signals through the generation of surface waves. It was found that a mixed impedance surface provided better amplification of acoustic signals than the lattice. Daigle and Stinson [5] also constructed a finite impedance surface using a strip of structured ground and found that the finite width of the strips gives rise to a directional response. This effect was exploited to obtain passive amplification. The sound pressure level was found to be 6 dB higher for

sound travelling parallel to the strips compared to sound travelling transversely. Bashir *et al* [6] investigated surface waves generated over arrays of parallel rectangular strips and found that the surface wave frequency decreased as the mean strip spacing was increased. The strips were regarded as a locally reacting rigid-framed hard-backed slit-pore layer with an effective depth slightly larger than the strip height when the spacing is close to the strip height. Although when the spacing is greater than the strip height, the slit-pore impedance model is no longer valid and the surface behaves more like a periodically rough surface.

The generation of air-borne acoustic surface waves is a problem in noise control and measures must be taken to reduce their effect. Passive amplification of acoustic signals through the generation of surface waves has also been investigated but studies into the control and use of surface waves for the purpose of signal enhancement is limited. This paper offers a numerical and experimental investigation into sound pressure level spectra with reference to a hard surface above periodically spaced rectangular strips. Laboratory measurements of excess attenuation with reference to an acoustically hard surface and time-domain measurements have been taken under anechoic conditions in order to study the nature and features of surface waves and the passive amplification achieved through their generation. These measurements are compared with numerical simulations using a two-dimensional boundary element method and a time-domain boundary element method.

2. Theory

A comb-like surface made from parallel rectangular strips can be considered to act acoustically as a hard-backed locally reacting rigid porous layer composed of slit-like pores [6]. The slit-pore impedance model is applicable where viscous and thermal boundary layers exist due to sound propagation between the slits. The ground may be characterised by a complex density $\rho(\omega)$, and a complex compressibility $C(\omega)$,which account for the viscous and thermal effects respectively.

$$\rho(\omega) = \frac{\rho_0}{H(\lambda)} \tag{1}$$

$$C(\omega) = \frac{1}{\gamma\rho_0}\left[\gamma - (\gamma - 1)H\left(\lambda\sqrt{N_{PR}}\right)\right] \tag{2}$$

$$H(\lambda) = 1 - \frac{\tanh\left(\lambda\sqrt{-i}\right)}{\lambda\sqrt{-i}}, \lambda = \sqrt{\frac{3\omega\rho_0 T}{\Omega R_s}} \tag{3}$$

The function $H(\lambda)$ is the complex density function, $\left(\gamma\rho_0\right)^{-1}$ is the adiabatic compressibility of air, γ is the ratio of specific heats, N_{PR} is the Prandtl number, Ω is the porosity and R_s is the flow resistivity. The dimensionless parameter λ can be related to the flow resistivity of the bulk material using the Kozeny-Carman formula,

$$R_s = \frac{2\mu T s_0}{\Omega r_h^2} \tag{4}$$

where T is the tortuosity (T = 1 for vertical slits), μ is the viscosity, s_0 is the pore shape factor (s_0 =1.5 for slit-like pores) and r_h is the hydraulic radius which can be taken to be half the value of the edge-to-edge spacing, between roughness elements.

The bulk propagation constant, $k(\omega)$ and the relative characteristic impedance, $Z_c(\omega)$ can be written as,

$$k(\omega) = \omega\sqrt{T\rho(\omega)C(\omega)} \tag{5}$$

$$Z_c(\omega) = \frac{1}{\rho_0 c_0}\sqrt{\left(\frac{T}{\Omega^2}\right)\frac{\rho(\omega)}{C(\omega)}} \tag{6}$$

3. Measurement

3.1 Measurement System

Measurements were carried out under anechoic conditions over periodically spaced rectangular aluminium strips placed on medium density fibreboard (MDF). The strips have a height of 0.0253m and width of 0.0126m. The source and receiver were separated by 0.75m and 1m. A Tannoy® driver and a detachable 2m long pipe, the end of which acts as a point source, was used and a Bruel & Kjaer type 4191 condenser microphone with a preamplifier as a receiver. A National Instruments USB-6529 data acquisition system was used for digital-to-analogue conversion. The excess attenuation spectrum was obtained by using a reference field as the 'direct' field. This reference field, P_{ref} was obtained by placing source and receiver as close to the ground as possible which shifts the ground effect minimum to a high frequency out of the range of interest. Aluminium strips were then laid on the MDF, spaced periodically by 0.02m. The source was placed at 0.045m above the MDF and the receiver height varied between 0.04m and 0.10m in 0.01m increments and a measurement of the total sound field over the strips P_{total} was obtained. The excess attenuation was calculated using,

$$EA = 20\log_{10}\left(\frac{P_{total}}{P_{ref}}\right) \tag{7}$$

The fact that the excess attenuation is measured relative to a hard surface rather than a free field means that the surface wave presence is indicated by an excess attenuation greater than 0dB in the data presented in this paper.

3.2 Input Signals

3.2.1 Maximum Length Sequence (MLS)

The MLS pulse was developed by Schroeder [7] as a method of measuring linear system responses without the use of impulses. The power spectrum of such a pulse is like that of a single impulse with a flat frequency response over a wide range of frequencies.

Pseudorandom noise is generated through periodic sequences of integers which take binary values of +1 or -1. The number of samples per period of length L of the MLS sequence depends on its order m:

$$L = 2^m - 1 \tag{8}$$

3.2.2 Ricker Pulse

The Ricker pulse (sometimes known as the Mexican hat wavelet) is a special case within the Hermitian wavelets. It is the second derivative of the Gaussian function and is given by,

$$\varphi(t) = \left(1 - \frac{t^2}{\sigma^2}\right)e^{-t^2/2\sigma^2} \tag{9}$$

$$\sigma = \frac{\sqrt{2}}{2\pi f} \tag{10}$$

where t is the period and eq.10 relates the spread, σ, to the centre frequency, f. The

Once the surface wave frequency is roughly known, this particular pulse is useful for studying surface waves in the time domain due to its narrow frequency band. For effective use of the Ricker pulse, the period must be greater than 10σ in order cover the whole pulse and achieve a resolution of σ.

4. Time-Domain Boundary Element Method (TBEM)

Surface waves may also be studied in the time-domain as later arrivals due to them travelling slower than the speed of sound in air. The boundary element method (BEM) solves partial differential equations formulated as boundary integrals. Through the implementation of boundary conditions, the sound field can be found at any point within a specified domain of interest. Taherzadeh et al [8] developed a 2-D BEM to predict sound propagation above an uneven boundary. This particular method solves the field equations in the frequency domain. To study surface wave arrivals, a time-domain BEM program has been developed.

A Fast Fourier Transform (FFT) can be calculated to obtain the frequency spectrum. The response in the time domain will be the Fourier integral of the product of the source function and the transfer function $p(r,z,\omega)$, obtained from the BEM simulation;

$$p(r,z,t)=\frac{1}{2\pi}\int_{-f_{nyq}}^{f_{nyq}} S(\omega)p(r,z,\omega)e^{-i\omega t}d\omega \tag{11}$$

where the maximum frequency is half the sampling frequency (Nyquist frequency, f_{nyq}). The source function $S(\omega)$ in this case, is a Ricker pulse. The fact that the solution to the Helmholtz wave equation is conjugate symmetric is used to account for the fact that it is not possible to integrate over negative frequencies;

$$p(r,z-\omega)=\overline{p(r,z,\omega)} \tag{12}$$

The inverse Fourier Transform can then be calculated for the full spectrum resulting in the time-domain response.

5. Results & Discussion

Measurements were conducted using a broadband MLS impulse in order to obtain excess attenuation spectra. Following that, a Ricker pulse with a centre frequency of 2500Hz was used over the same geometry in order to study the observed surface waves in the time-domain.

5.1 Measurement

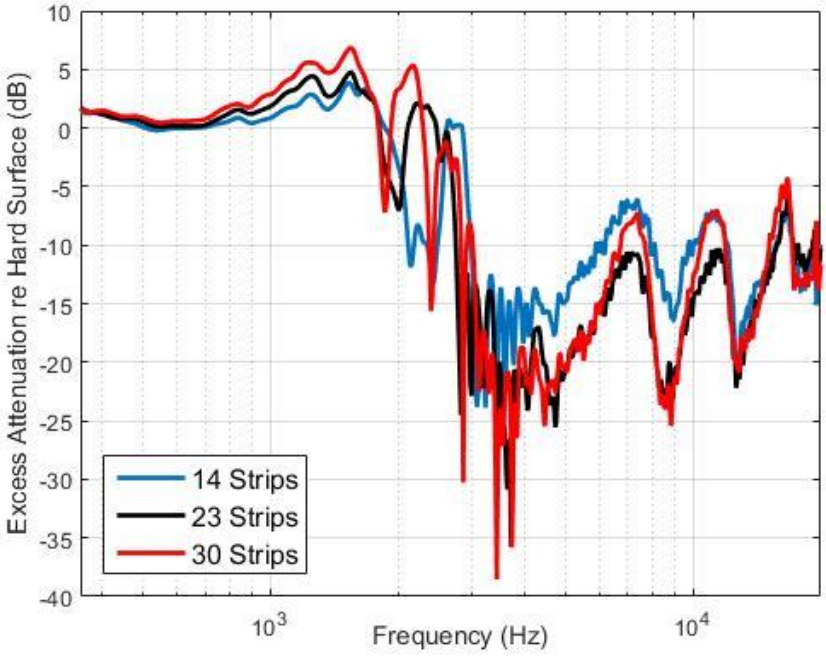

Figure 1: Excess attenuation spectrum obtained over 14, 23 and 30 periodically spaced rectangular strips; covering 0.50m, 0.75m and 1.00m respectively, using an MLS impulse as the input. The source-receiver distance was kept constant at 1.00m.

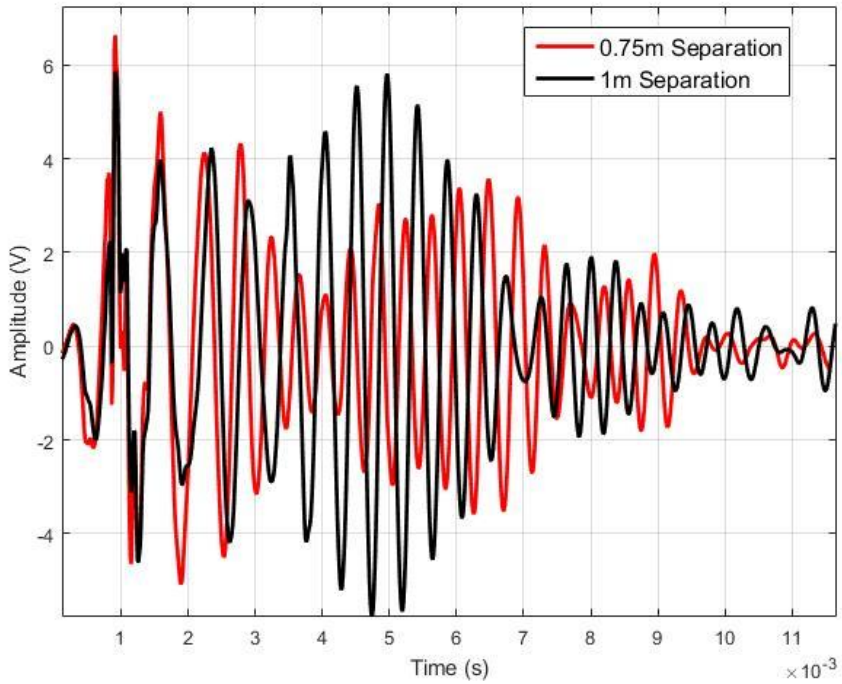

Figure 2: Time-domain data obtained using a Ricker pulse over 30 periodically spaced rectangular strips with a source-receiver separation of 0.75m and 1.00m. The centre frequency of the Ricker pulse is 2500Hz.

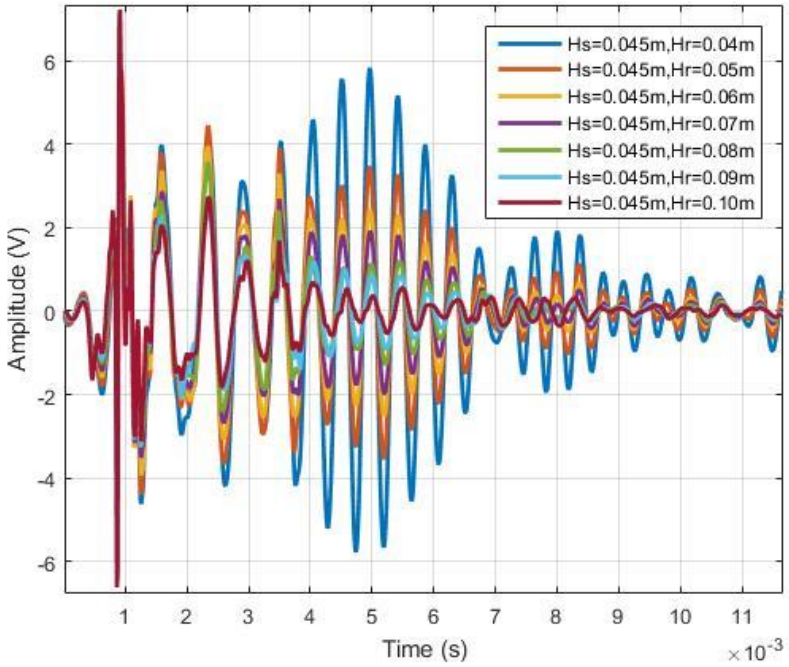

Figure 3: Time-domain data obtained using a Ricker pulse over 30 periodically spaced rectangular strips covering 1.00m. The receiver height is varied between 0.04m and 0.10m and the source height is kept constant at 0.045m.

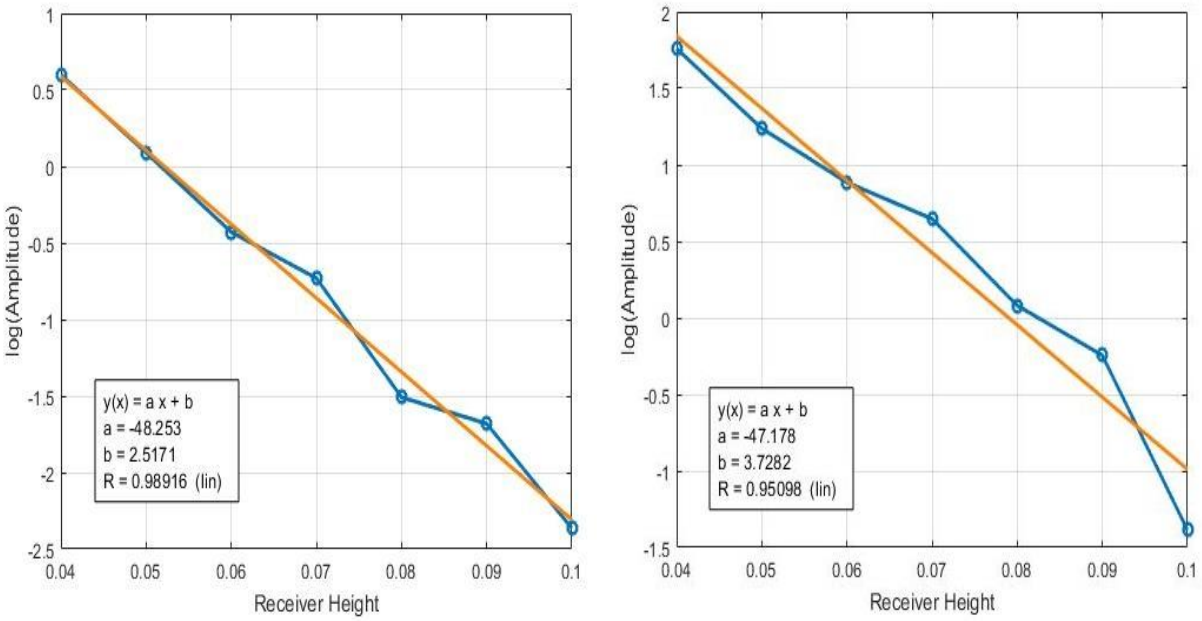

Figure 4: The logarithm of the amplitude plotted against receiver height for the maximum at 8.37ms (left) and 4.96ms (right). The surface wave amplitude decays exponentially with height so the presence of surface wave at these points is indicated by the linear relationship shown above. The gradient, a, above is the attenuation constant. The fact that they are almost equal is further prove for the presence of a surface wave.

Figure 1 shows a distinct peak up to 7 dB compared with the excess attenuation over a hard surface for all 3 strip arrays at 1548Hz which is associated with a surface wave. This along with the alignment of peaks in figure 3 indicate that receiver height has no effect on the frequency of the surface wave, only the amplitude as shown in figure 4. Multiple surface wave peaks have been noted by Daigle and

Stinson [5] and attributed to interference with reflections from the edges of the finite array in the source-receiver direction.

The time-domain data displayed in figure 3 has been shifted so that the direct arrivals occur simultaneously in time at 0.91ms. This allows the surface wave components to be studied in more detail. The frequency of the excess attenuation maximum discussed above is 1841Hz which corresponds, roughly, to the frequency of the time domain peaks at 2.35ms. This suggests that these peaks are associated with the surface wave arrival at the receiver since it travels at slightly less than the speed of sound in air. However, more precise measurements over greater distances are required to achieve higher resolution of the surface wave arrival. The average frequency of the next (more distinct) wave train between 2.90ms and 7.65ms is 2233Hz and that of the further wave train between 7.29 ms and 9.47 ms is 2695Hz. These wave trains correspond to the features above 0 dB present at 2174Hz, 2266Hz and 2653Hz for the 30, 23 and 14 strip arrays respectively to within the 40 Hz uncertainty calculated by taking the uncertainty in time to be half the sampling rate. This suggests separate features which are not constant in frequency or time and therefore cannot simply be the result of interference from reflections due to the finite depth of the array in the source-receiver direction.

5.2 Time-Domain Boundary Element Method (TBEM) Simulations

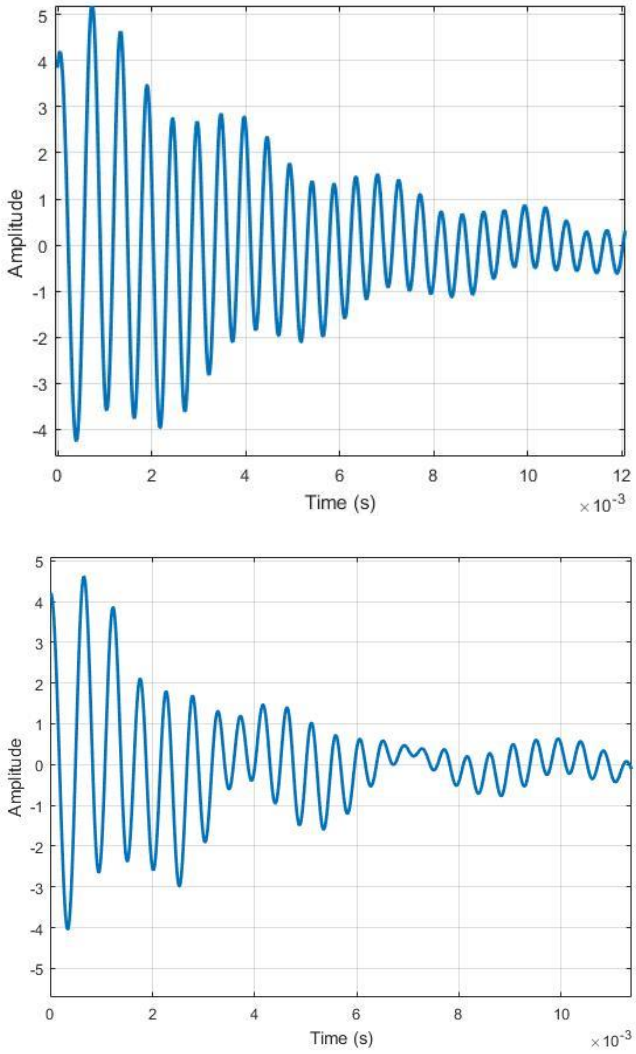

Figures 5 & 6: Output from TBEM simulations of sound propagation over 30 periodically spaced strips separated by 0.02 m (as in measurement) using a Ricker pulse as the source function. The source and receiver are separated by 1.00 m (top) and 0.75 m (bottom) and are at a height of 0.45 m and 0.04 m respectively.

The frequency of each wave displayed in the BEM simulations for both source-receiver distances are between 2155Hz and 2283Hz which is further confirmation that the peaks shown in the measured excess attenuation spectra are due to a physical effect. These results also lie within the ±40 Hz uncertainty since the same sampling rate is used throughout. It should be noted that the BEM program is a 2-D simulation and therefore do not include any effects due finite strip width.

6. Conclusions & Future Work

Experiments and numerical simulations have shown that arrays of regularly spaced rectangular strips are efficient generators of surface waves. However they have been found to give rise to further surface wave like effects at slightly higher frequencies. It is clear, from the results displayed through measurement of excess attenuation, time-domain data and outputs from a time-domain boundary element method that these later arrivals in the time-domain are not simply reflections due to the finite depth of the array in the source-receiver direction. Further measurements and simulations are planned to investigate this further.

REFERENCES

1. T.L. Richards, K. Attenborough (1989), Solid Particle Motion Induced by a Point Source Above a Poroelastic Half-Space, *Journal of Acoustical Society of America*, vol **86 (3)**, p1085 – 1092

2. J.F. Allard, G. Jansens, G. Vermeir, W. Lauriks (2002), Frame-Borne Surface Waves in Air-Saturated Porous Media, *Journal of Acoustical Society of America*, vol **111** (2), p690

3. C. Hutchinson-Howorth, K. Attenborough (1992), Model Experiments on Air-Coupled Surface Waves, *Journal of Acoustical Society of America*, vol **92 (4)**, p2431

4. W. Zhu, G.A. Daigle, M.R Stinson (1996), Experimental and Numerical Study of Air-Coupled Surface Waves Generated Above Strips of Finite Impedance, *Journal of Acoustical Society of America*, vol **99 (4)**, p1993

5. G.A. Daigle, M.R Stinson (2004), Passive Amplification and Directivity from Air-Coupled Surface Waves Generated Above a Structured Ground, *Journal of Acoustical Society of America*, vol **115 (5)**, p1988 – 1992

6. I. Bashir, S. Taherzadeh, K. Attenborough (2013), Surface Waves Over Periodically-Spaced Rectangular Strips, *Journal of Acoustical Society of America*, vol **134 (6)**, p4691 – 4697

7. M.R. Schroeder (1979), Integrated-Impulse Method for Measuring Sound Decay Without Using Impulses, *Journal of Acoustical Society of America*, vol **66 (2)**, p496

8. S. Taherzadeh, K.M Li, K. Attenborough (2001), A Hybrid BIE/FFP Scheme for Predicting Barrier Efficiency Outdoors, *Journal of Acoustical Society of America*, vol **110 (2)**, p918